Optical Absorptivity and Thermal Property of LPCVD-Deposited Low-Stress Si-Rich Nitride Membrane for Far-Infrared Sensor

Fabio Jutzi, Dedy H.B. Wicaksono, Grégory Pandraud, and Paddy J. French

***Abstract*—This paper reports our investigation on the 8-14 μm wavelength region optical absorptivity and thermal property of low stress Si-rich Nitride (SiN) membrane deposited using Low-Pressure Chemical Vapor Deposition (LPCVD) method. Although the use of Si_xN_y membrane material as far-infrared radiation absober have been reported in many papers (e.g. [1, 2]), yet there are still few report addressing its fundamental optical absorption property at this wavelength region, in relation with its thermal properties, utilized in an infrared sensing device. Although such properties are very process-dependent, we are trying to devise a general rule and method of combining both theoretical simulations and experimentally-observed data, for obtaining such properties, which in turn, enabling better design and optimization of the Infrared device, especially when scaling down is an issue. Results show that the absorptivity depends on the thickness of the SiN thin film, yet all the samples show absorption selectivity at 8-14 μm, with up to 50% absorption. Thermal sensitivity also depends on the membrane size. A 1000x1000 μm^2 will achieve 80K/(Wcm^{-2}), while membrane as small as 10x10 μm^2 has only 0.15 to 0.3 K/ (Wcm^{-2}). Yet faster time response is understandably obtained in the smaller size membrane. All this issues need to be optimized, and addressed to have the best absorber membrane options for particular far infrared sensing applications.**

***Index Terms*— Far Infrared Radiation (FIR), Infrared sensor, LPCVD, MEMS, SiN**

I. Introduction

Far Infrared (FIR) sensor capable of detecting infrared radiation at 8-14 μm or longer is normally used in thermal imaging application, night vision application, as well as astronomical observation. Current infrared (IR) sensor devices consist mostly of photodetector devices, and thermal detector devices. Photodetector devices are made of compound semiconductor having bandgap related to infrared radiation. Although this type of device has high sensitivity and fast response, its high production-/operational- cost and its sharp bandwidth, have limited its applications to very specific advanced fields like astronomy. The high operational cost of such photodetector IR sensor is due to the need of cooling to suppress thermal intrinsic noise. Thermal detectors, on the other hand, use indirect signal conversion from optical to thermal to electrical, or via mechanical signals. It has lower cost, and broader bandwidth, enabling it to be used in broader applications both in military and civilian application fields. A review of different kinds infrared sensor can be read in ref. [3].

In thermal detector-type IR sensor, an important transducer element is the thermal absorber, whose function is to convert radiation signal at particular wavelength bandwidth onto thermal signal, hence temperature change. This temperature change can further be converted into electrical signals using well-known temperature transducer, e.g. thermistor, thus forming a resistive bolometer [cf. 4]; pyroelectric material [cf. 5]; or thermoelectric material, i.e. thermopile [cf. 1, 6]. The remaining heat is then channeled to a constant temperature heat sink. Typical configuration of IR thermal detector is illustrated in figure 1.

Different absorber materials have been used for IR thermal detectors. The black metal absorbers [3], constituting porous metal with thicknesses of several micrometers [7] is often being used as a wideband absorber. In other papers thin metal film absorbers are reported as infrared absorbers [8,9]. This

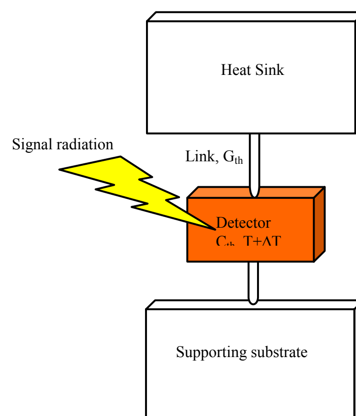

Fig. 1. Typical Infrared thermal detector configuration

This work was supported in part by the Dutch Technological Foundation (STW) under Grant DEL. 6050.

F. Jutzi was with Section de Microtechnique, Ecole Polytechnique Fédérale de Lausanne, Switzerland.

D.H.B. Wicaksono, G. Pandraud, and P.J. French, are with Electronic Instrumentation Lab., Dept. of Microelectronics, DIMES, Delft University of Technology, Mekelweg 4, 2628CD, Delft, The Netherlands (e-mail: {d.h.b.wicaksono@tudelft.nl).

thin metal films, often nickel, has a specific sheet resistance matching the free space impedance. Depending on the thickness, which are in the range of tens of nanometers, the absorptance is usually around 50%. The absorptance can be broadband or selective for a narrow wavelength-bandwidth. Combining a quarter wavelength resonance cavity with a thin metal film gives absorption of 100%, a principle described in [10]. Silicon nitride (Si_xN_y) is also being reported to be used as infrared absorber for sensors, since it seems to be absorbing in the 8-14 μm wavelength region [1,2,11]. Unfortunately the exact optical constants for silicon nitride are not exactly known in the far infrared region. They might be also quite varying depending on the deposition process like shown in [12]. The usage Si_xN_y membrane material as far-infrared absober has several advantages: compatibility to CMOS processing, low-cost, good mechanical property. Yet, despite these advantages, and despite its growing use as absorber material, there are still few report addressing its fundamental optical absorption property at this wavelength region, in relation with its thermal properties, utilized in an infrared sensing device.

In this paper, we try to devise a general rule and method of combining both theoretical simulations and experimentally-observed data, for obtaining such properties, which in turn, enable better design and optimization of the infrared device, especially when scaling down the size is an issue.

Here, a theoretical model of dielectric materials' optical properties was obtained from literatures. Measurements, both in a custom set-up (fig. 2), and FTIR (Fourier Transform Infrared) Spectroscopy, were conducted to get optical transmission and reflection data of particular SiN thin films. Based on this data, numerical calculation was performed to obtain the model's parameters. The resulted model was again confirmed with optical measurements from a fabricated SiN membrane. Thermal property was modelled both analytically and numerically, to know its steady state temperature increase, as well as its thermal time constant. Experiments measuring temperature increase on the fabricated thermistor on the membrane, due to, both, controlled heating and incoming infrared radiation, were conducted to verify the models.

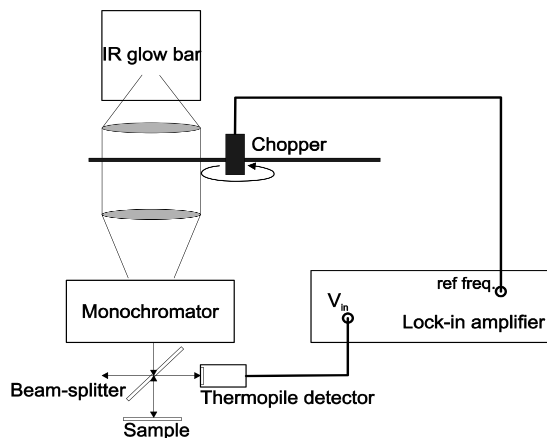

Fig. 2. Measurement setup for reflectance measurements using a monochromator. For transmittance measurement the same setup was used, but the sample was put directly at the output slit of the monochromator. The thermopile detector was then placed for this case just behind the sample.

II. Theoretical Modelling

A. Absorption in Dielectric Materials

The optical properties of a dielectrical absorbing layer is given by its complex refractive index $\tilde{n} \equiv n + ik$, where *n* is the refractive index and *k* the extinction coefficient [13]. The amplitude of an electromagnetic wave propagating in z direction is given by the following formula [13]:

$$U(z) = U_o e^{i\frac{2\pi}{\lambda}\tilde{n}z} = U_o e^{i\frac{2\pi}{\lambda}\tilde{n}z - \frac{2\pi}{\lambda}kz} \quad (1)$$

The power (intensity) of the propagating electromagnetic wave in z direction then is given as the square value of the real part of the wave amplitude given in the above mention:

$$I(z) = C\left|\mathrm{Re}\{U(z)\}\right|^2 = I_0 e^{-\frac{4\pi}{\lambda}kz} \quad (2)$$

where I_0 is the initial power at z = 0. The power transmitted through the dielectric material (see figure 3), I_t, is given by the product of the transmittance T and I_0.

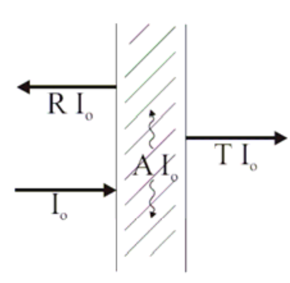

Fig. 3. Incident radiation I_0 passing through a medium with a reflectance R, absorptance A, and transmittance T

The following relation is then valid for the radiation passing a dielectric material as illustrated in fig.2: *R+A+T=1* [14]; Then the absorption *A* can be calculated from measured/calculated *Transmittance T* and measured/calculated *Reflectance R*:

$$A = 1 - R - T \quad (3)$$

All these parameters *R*, *T*, and *A* are dependent on the optical properties of the material. Thus, by calculating and/or measuring *R* and *T*, we would be able to estimate and calculate the value of absorption at particular wavelength for a dielectric material with particular structural parameters (e.g. thickness).

B. The Lorentz Oscillator Model

In order to be able to calculate material optical parameter constants from reflection or transmission measurements, a mathematical model that correlates reflection and transmission data as functions of wavelength and the material optical properties, is needed. Hence, for dielectric material e.g. Silicon nitride and silicon oxide, the Lorentz Oscillator can be used [15]. The model gives the change of complex dielectric

constant as a function of wavenumber (reciprocal of the wavelength), and in turn this complex dielectric constant will determine the value of the complex refractive index. The reflection and refraction depends on this complex refractive index. Thus, if the dielectric constant ε is expressed as $\varepsilon = (\varepsilon' + i\varepsilon'')$, then:

$$\varepsilon' = \varepsilon_\infty + \frac{F(\sigma_0^2 - \sigma^2)}{(\sigma_0^2 - \sigma^2)^2 + (\Gamma\sigma)^2} \qquad \varepsilon'' = \frac{F(\Gamma\sigma)}{(\sigma_0^2 - \sigma^2)^2 + (\Gamma\sigma)^2} \tag{4}$$

where Γ is the half width of the ε″ peak and σ_0 is the resonance wavenumber, that means at the maximum absorbance; and *F* is a constant parameter that can be expressed as: $F = (\varepsilon_0 - \varepsilon_\infty)\sigma_0^2$, where ε_0 is the dielectric constant when the frequency approached zero and ε_∞ is the dielectric constant for high frequencies. The wavenumber σ is given with the unit cm^{-1}, and related to the wavelength λ in μm with the following equation:

$$\sigma[cm^{-1}] = \frac{10000}{\lambda[\mu m]} \tag{5}$$

Then the complex refractive index $\tilde{n} = n + ik$ can be calculated as a function of ε as follows:

$$n = \left[\tfrac{1}{2}\left(\sqrt{\varepsilon'^2 + \varepsilon''^2} + \varepsilon'\right)\right]^{\frac{1}{2}} \qquad k = \left[\tfrac{1}{2}\left(\sqrt{\varepsilon'^2 + \varepsilon''^2} - \varepsilon'\right)\right]^{\frac{1}{2}} \tag{6}$$

C. Heat Conduction Theory

After the infrared radiation is absorbed by the membrane absorber, we have to be able to calculate and estimate the temperature increase and its distribution within the absorber material, as well as in the surrounding sink region of the sensor. Here, we will review the heat conduction equation [16] applied for our case, i.e. the membrane absorber in the sensor.

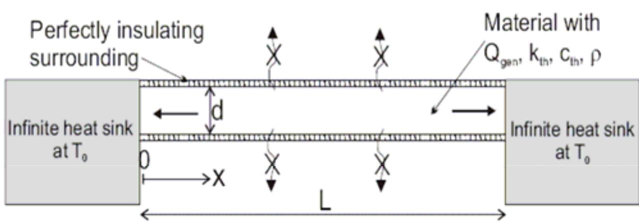

Fig. 4. 2-D simplified structure model of the SiN membrane for heat conduction modelling

To simplify the analysis, the membrane structure is evaluated as 2-dimensional structure with thickness *d* and length *L* [m] as illustrated in the figure 4.

The material has a thermal conductivity of k_{th} [W/(m.K)], thermal capacitance c_{th} (J/(kg.K)), and density ρ [kg/m^3]. Here, the infrared radiation heat being absorbed is simulated as a heat source Q_{gen} generated in the structure per unit volume per unit time. The structure is surrounded by an infinite heat sink, which has a constant temperature T_0, similar to the ambient temperature.

The heat equation for conduction in one dimension x is given [16] as the following:

$$\rho c_p \frac{\partial T}{\partial t} = k_{th} \frac{\partial^2 T}{\partial x^2} + Q_{gen} \tag{7}$$

where *T* stands for temperature, and *t* for the elapsed time. For steady-state response, we have the first term $\frac{\partial T}{\partial t} = 0$. Thus, eq. 7 becomes eq. 8 as follows:

$$Q_{gen} = -k_{th} \frac{\partial^2 T}{\partial x^2} \tag{8}$$

By putting the boundary condition of temperature T_0 at the boundaries between the membrane and the sink, we solve the above steady-state equation as follows:

$$T(x) = \frac{Q_{gen}}{2k_{th}}(Lx - x^2) + T_0 \tag{9}$$

The maximum temperature is at x = L/2, i.e. in the middle of the membrane:

$$T_{\max} = \frac{Q_{gen}}{8k_{th}} L^2 + T_0 \tag{10}$$

To calculate the thermal time constant, we proceed from eq. 7, by assuming that there is no heat generation, since we would like to know the cooling time:

$$\rho c_p \frac{\partial T}{\partial t} = k_{th} \frac{\partial^2 T}{\partial x^2} \tag{11}$$

If we assume that temperature T is a product of a function X which is only dependent in x, and another function Θ which is only dependent to t,

$$T(x,t) = X(x).\Theta(t) \tag{12}$$

Then, eq. 11 can be modified by eq. 12 to become eq. 13 as follows:

$$\frac{\rho c_p}{k_{th}} \frac{1}{\Theta} \frac{\partial \Theta}{\partial t} = \frac{1}{X} \frac{\partial^2 X}{\partial x^2} \tag{13}$$

The solution of this differential equation is:

$$\Theta(t) = C_1 e^{-\mu \frac{k_{th}}{\rho c_p} t} = C_1 e^{-\frac{t}{\tau}} \tag{14}$$

The temperature will drop exponentially with a time constant $\tau = \frac{\rho c_p}{\mu k_{th}}$. To obtain μ, we use the steady state solution, that depends only to the distance x from the previous equation 8. By inserting the steady-state solution, we achieve the following solutions:

$$\mu = \frac{2}{(Lx - x^2)} \tag{15}$$

For example, at the centre of the membrane where x = L/2, the time constant is calculated to be of:

$$\tau = \frac{\rho c_p}{8 k_{th}} L^2 \qquad (16)$$

III. EXPERIMENTAL

A. Reflection and Transmission Measurement

The samples used consist of LPCVD SiN deposited onto a silicon substrate. The substrate was a 10 cm diameter crystalline silicon wafer polished on one side. The deposition was carried out on the polished side. Two thicknesses of LPCVD SiN thin films were used for the measurements: 500nm and 200nm. Transmission and Reflection (30°) measurements were carried out using two methods: Monochromator, and FTIR (Fourier Transform Infrared) Spectrometer.

B. Heat Conduction Numerical Simulation

1) Steady-State Temperature Distirbution on the Membrane

The cross section of a SiN membrane on top of a Si wafer is simulated in air. The geometry of the simulated system is similar to the one shown in fig. 4. The membrane has a sidelength *L*, which was varied from 1000 µm to 10 µm. The thicknesses *d* simulated were 1000 nm, 600 nm and 300 nm. Even when in the real fabrication, the Si-nitride membrane covers the whole wafer, a finite width of *w* was chosen for the simulations. The reason was to lower computational time. Preliminary simulations showed that since the thermal conductivity of Si is much higher than that of SiN there is no temperature increase of the nitride where it is directly on the silicon substrate. The SiN layer width is set to 2.5 mm for membrane sizes of 1000 µm and 500 µm and to 0.25 mm for smaller membrane sizes. In the whole system the initial temperature is set to T_0 equal to 273.15 K. Whereas the outer boundary has this temperature as a constant. In the rest of the system the temperature can vary. The upper boundary of the SiN layer was set to being a heat source of q_0, which was arbitrary chosen to be $1 W/cm^2$. The material proprieties can be seen in table 1.

TABLE I
MATERIAL PROPERTIES USED IN SIMULATION

Material	k_{th}, Thermal conductivity [W/m.K]	ρ, Density [kg/m^3]	Cp, Thermal capacitance [J/kg.K]
Si	130	2329	700
SiN	1.55 [18]	2400 [19]	700
Air	0.024 [20]	1 [20]	1006 [20]

2) Transient Temperature Increase on the Membrane

To obtain the thermal time constant, the SiN layer is set at 100 K higher temperature than the rest of the system and then the decay rate of its temperature is calculated. Here again the same system in fig. 4 was used. But, the initial and boundary conditions were changed. This means the initial temperature of the membrane layer was set to 373.15 K this is 100 K higher than the rest of the system. All boundaries were set to continuity, except the outer one which has again a constant temperature of 273.15 K. That means no heat source was introduced to the system. A transient linear analysis was performed for a time interval long enough to have a temperature decrease of the SiN to the surrounding temperature. The temperature data from the central point of the membrane as a function of the time was extracted from COMSOL. Subsequently the exponential decay function from the equation derived in previous sections was fitted to the data using Matlab. The time constant is obtained out of this fitted exponential function.

C. Test Structure Fabrication and Measurement

The test device is a membrane with a temperature sensor placed on it. As temperature sensor, a resistor with a high temperature coefficient of resistance is chosen. By measuring the change of the resistor value, the temperature of the membrane can be obtained. Polysilicon and platinum are used as thermistor material. As membrane material we will use silicon nitride, deposited with LPCVD (Low-Pressure Chemical Vapour Deposition), thus a low stress membrane can be obtained, which is important when it is desired to build large membranes. Different membrane sizes are fabricated, so the dependency of the sensitivity on the size of the sensor can be evaluated. The membrane is fabricated with bulk micromachining: A SiN coated Si wafer is back side

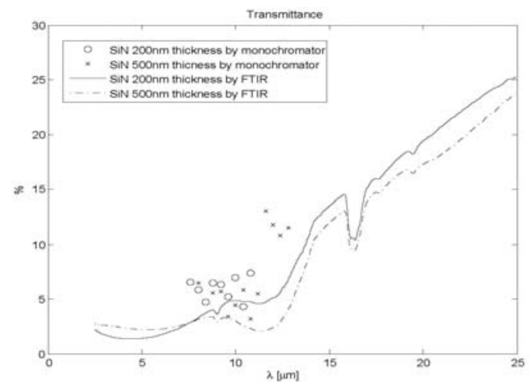

Fig. 5. Transmission Measurement Results

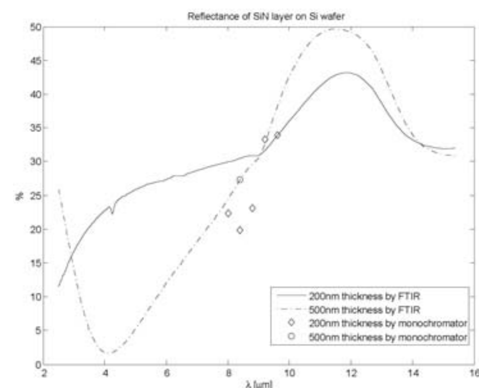

Fig. 6. Reflection Measurement Results

anisotropically etched with etch stop on the nitride membrane.

IV. RESULTS AND DISCUSSION

A. Reflectance-Transmittance Measurement and Absorption Calculation

Transmitance measurement of SiN membrane, using FTIR spectrometer and the monochromator setup explained in previous section, is shown in figure 5. Reflectance measurement result of SiN layers deposited on Si wafer (525 μm thickness) using FTIR (at 30° angle) and monochromator setup, are shown in figure 6.

By using the measured reflectance data, and initial guess for the constants of the Lorentz oscillator model (eq. 4), i.e. (ε_0, ε_∞, Γ, σ_0), an iterative algorithm was carried out to obtain these coefficient with a relatively small end-error. The obtained Lorentz Oscillator coefficients based on the reflectance measurement of 500 nm and 200 nm SiN membrane are as shown in table 2.

TABLE 2
MATERIAL PROPERTIES USED IN SIMULATION

Membrane Thickness	ε_∞	ε_0	Γ	σ_0	Error*
500 nm	4.68	7.3	147	858	0.621
200 nm	4.49	8.2	205	845	0.516

*Mean square error between fitted and measured values as percentage of reflectance

Then by using *n* and *k*, calculated from these Lorentz' coefficients, absorptance of SiN membrane from different thicknesses are calculated, and shown in figure 7.

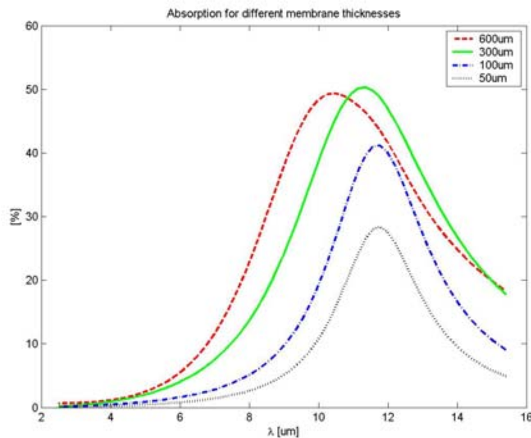

Fig. 7. Calculated Absorptance of SiN membrane

B. Heat Conduction Simulation Result

The temperature distribution of a 1000 nm thick SiN membrane with 1000 μm side-length, with a heat flux of 1 W/cm^2 is shown in figure 8. Sensitivity of the SiN membrane as a function of its side-length and thickness, is shown in figure 9. The calculated results coincide simulated results at small side-length. This is understandable, since at bigger size, there are other factor unaccounted for, e.g. convection. While

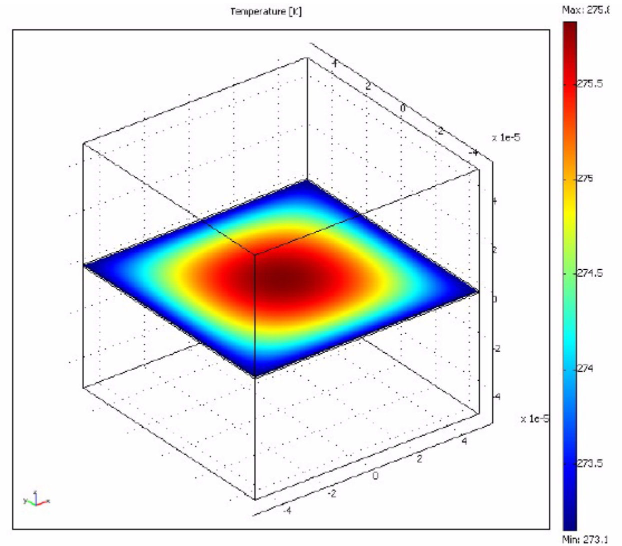

Fig. 8. 2-D temperature distribution across the SiN membrane

decreasing the length, will decrease the sensitivity, decreasing the thickness on the other hand, will increase sensitivity.

Thermal time constant as a function of membrane size for different thickness is plotted in figure 10. As expected, the time constant decrease, as the thickness and the side-length decrease. The discrepancy found between the numerical simulation result and analytical result, at large side-length is due to the assumption made in the derivation of the analytical solution.

V. CONCLUSION

The optical absorption properties of SiN membrane at Far Infrared radiation region have been simulated and measured. The absorptivity depends on the thickness of the SiN thin film. Yet, all the samples show absorption selectivity at 8-14 μm, with up to 50% absorption. The results shows promising potentials of SiN membrane to be used for the novel bio-inspired FIR sensor, fabricatable using CMOS-compatible

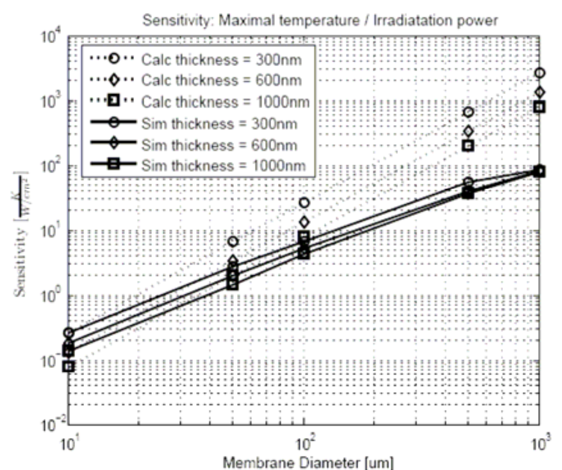

Fig. 9. Sensitivity of the SiN membrane as function of thickness and side-length

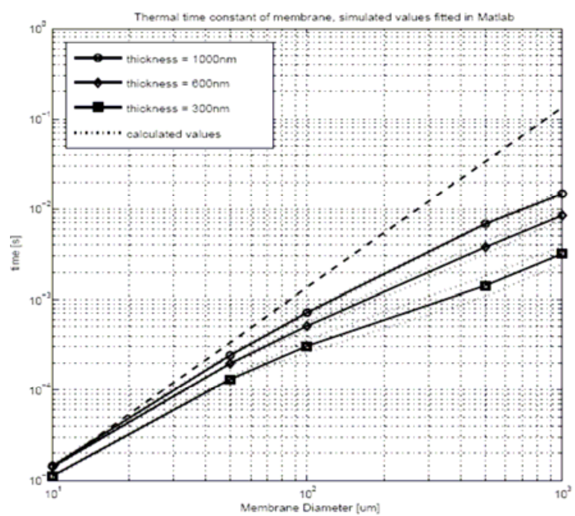

Fig. 10. Thermal Time constant, calculated and numerically simulated for membrane with different size and thickness

processing. The heat conduction mechanism has also been simulated to predict maximal temperature change, and thermal time constant. Thermal sensitivity depends on the membrane size. A 1000x1000 μm^2 will achieve 80K/(Wcm^{-2}), while membrane as small as 10x10 μm^2 has only 0.15 to 0.3 K/ (Wcm^{-2}). Faster time response is understandably obtained in the smaller size membrane, as expected from analytical model. A test structure of the real SiN with thermal-sensitive resistor has been fabricated. Results show that a 10x10 μm^2 membrane has a good (i.e. fast) thermal response.

ACKNOWLEDGMENT

The authors would like to thank technicians and staff of DIMES for their assistance in the sample fabrications.

REFERENCES

[1] R. Lenggenhager, D. Jaeggi, P. Malcovati, H. Duran, H. Balter, and E. Doering, CMOS Membrane Infrared Sensors and Improved TMAHW Etchant, in *Proc. of IEEE Intl. Electronics Dev. Meetings 94-531,* 1994, pp. 20.5.1-20.5.4.

[2] A.J.L. Adam, T.O. Klaassen, J.N. Hovenier, and P.M. Sarro, Design and fabrication of a novel room temperature Terahertz detection array, in *Procs. Of Joint 29th Intl. Conf. on Infrared and Millimeter Waves and 12th Intl. Conf. on Terahertz Electronics*, 2004, pp. 755-756.

[3] A. Rogalski, Review: Infrared detectors: status and trends, in *Progress in Quantum Electronics*, 2003, **27**, pp. 59-210.

[4] K.C. Liddiard, Thin-film Resistance Bolometer IR detectors, in *Infrared Phys.*, **24** (1)**,** 1984, pp. 57-64

[5] D.Lienhard, F. Heepmann, and B. Ploss, Thin nickel film as absorbers in pyroelectric sensor arrays, in *Microelectronic Engineering*, **29**, 1995, pp. 101-104

[6] M.C. Foote, E.W. Jones and T. Caillat, Uncooled thermopile infrared detector linear arrays with detectivity greater than 10^9 cmHz$^{1/2}$/W, in *IEEE. Trans. On electron devices* 45 (9), 1998, pp. 1896-1902.

[7] W. Becker, R. Fettig, W. Ruppel, Optical and electrical proprieties of black gold layers in the far infrared, Infrared Physics and Technology 40 (1999), pp. 431-445

[8] D. Lienhard, F. Heepmann, and B. Ploss, Thin nickel film as absorbers in pyroelectric sensor arrays, *Microelectronic Engineering*, 1995, 29: 101-104

[9] S. Bauer, S. Bauer-Gogonea, W. Becker, R. Fettig, B. Ploss, and W. Ruppel, Thin metal films as absorbers for infrared sensors, *Sensors and Actuators A*, 1993, 37-38: 497-501

[10] M.P. Thompson, J.R. Troxell, m.E. Murray, C. M. Thrush, J.V. Nantese, Infrared absorber for pyroelectric detectors, J. Vac. Sci. Technol. A 25 (3), 2007, p. 437-440

[11] F. Ferrieu, Infrared spectroscopic ellipsometry using a Fourrier transform infrared spectrometer: Some applications in thin/film characterization, Rev. Sci. Instrum Vol. 60, No. 10, October 1989

[12] P.J. French, Optimization of a low-stress silicon nitride process for surface-micromachining applications, Sensors and Actuators A 58 (1997), pp. 149-157

[13] R. Kunz, Lecture Notes “Integrated Optics”, Master Course for Microtechnique students at EPFL, 2006

[14] E. Hecht, Optics, 4th Ed., Pearson Education, 2002.

[15] Ernst Heiner Korte, and Arnulf Röseler, Infrared reststrahlen revisitied: commonly disregarded optical details related to *n*<1, *Anal. Bional.Chem.*, 2005, 382: 1987-1992

[16] M. Jakob, Heat Transfer, Volume 1, John Wiley & Sons, 1955

[17] Oriel Instruments, The Book of Photon Tools, Catalogue 1999, pp. 4-56

[18] A. Irace, P.M. Sarro, Measurement of thermal conductivity and diffusivity of single and multi-layer membranes, *Sensors and actuators A.*, 1999, vol. 76, no. 1-3, 323-328

[19] Y. Zhao, M. Mao, R. Horowitz, A. Majumdaar, J. Varesi, P. Norton, J. Kitching, optomechanical Uncooled infrared Imaging System: Design, microfabrication, and Performance, *J. of Microelectromechanical Sys*. Vol. 11 No. 2 April 2002, pp. 136-146

[20] P. Renaud, lecture notes, “Scaling in MEMS”, *Master course for Microtechnique students at EPFL*, chapter II, Thermal Effects, 2006.

Fabio Jutzi was a Master of Science student at Section de Microtechnique, Ecole Polytechnique Fédérale de Lausanne, Switzerland. His main interest is in Nanotechnology and Microsystem. The results presented in this paper come from his graduation project that he carried out at Electronic Instrumentation Lab., Dept.of Microelectronics, Delft University of Technology, the Netherlands, under the supervision of Dedy H.B. Wicaksono, and Prof. Paddy French.

Dedy Hermawan Bagus Wicaksono was born in 1974 in Surabaya - Indonesia. He got his B.Eng degree, with honour (cum laude), from the Department of Engineering Physics, Bandung Institute of Technology (ITB Bandung), Indonesia. He got his M.Eng in Biological Information Engineering from the Tokyo Institute of Technology, Japan, in September 2002. He is currently finishing his PhD work within Electrical Instrumentation Laboratory at Delft University of Technology under the supervision of Prof. Paddy J. French. His main research interests are Biomimetic Sensors, Physical Biosensors, and MEMS.

Grégory Pandraud was born in Lyon, France in 1971. He received the Ph.D. degree in optics, optoelectronics from the University of Saint-Etienne, France in 1998 and then joined the University of Twente, The Netherlands, as postdoctoral fellow for one year. His work was then focused on optical sensors for mTAS devices. From 1999 to 2002 as Development Engineer and Senior Design Manager respectively with Bookham Technolgies plc., UK, and Opsitech S.A., France, he developped integrated optical components for DWDM and next generation networks applications. He joined Electronics Instrumentation of TU Delft in 2003 where he now works on development of post processing micromachining modules.

Paddy French was born in Rochford, England, in 1960. He received his B.Sc. in mathematics and M.Sc. in electronics from Southampton University, UK, in 1981 and 1982, respectively. In 1986 he obtained his Ph.D., also from Southampton University, which was a study of the piezoresistive effect in polysilicon. He then spent 18 months at Delft University of Technology, on the Royal Society European Exchange Programme, investigating new flip-flop sensor structures. In 1988 he moved to Japan and worked for 3 years in the Central Engineering Laboratories of Nissan Motor Company on sensors for automotive applications.

He returned to Delft University of Technology to begin a three year FOM sponsored fellowship at the Laboratory for Electronic Instrumentation to study micromachining. Since 1994, he is one of the project leaders of this laboratory. His main research interests are silicon technology, mechanical sensors and actuators, MOS-based sensors and process optimisation related to sensors. In 1999 he was awarded the Antoni van Leeuwenhoek chair. In 2002 he became head of the Electronic Instrumentation laboratory.